A Perspective on the 40-Year History of FDTD Computational Electrodynamics

Allen Taflove

Department of Electrical Engineering and Computer Science
Northwestern University
Evanston, IL 60208

Abstract — This paper arises from an invited plenary talk by the author at the 2006 Applied Computational Electromagnetics Society Symposium in Miami, FL (The 71 original slides can be downloaded at `http://www.ece.northwestern.edu/ecefaculty/taflove/ACES_talk.pdf`). This paper summarizes the author's perspectives on the history and future prospects of finite-difference time-domain (FDTD) computational electrodynamics on the occasion of the fortieth anniversary of the publication of Kane Yee's seminal Paper #1. During these four decades, advances in basic theory, software realizations, and computing technology have elevated FDTD techniques to the top rank of computational tools for engineers and scientists studying electrodynamic phenomena and systems.

I. INTRODUCTION

In May 1966, Kane Yee published the first paper to delineate the space and time discretizations of Maxwell's equations which form the basis of the finite-difference time-domain (FDTD) method [1]. As of March 7, 2006, according to a search conducted by the author on the ISI Web of Science®, Yee's paper had been cited 2441 times since its publication. This large number of citations is a quantitative measure of the seminal nature of Yee's insights, which opened the door to an entirely novel approach to computational electrodynamics relative to the other techniques being used by engineers and scientists in 1966. As shown in Fig. 1, the growth in FDTD-related publications continues unabated to the present time.

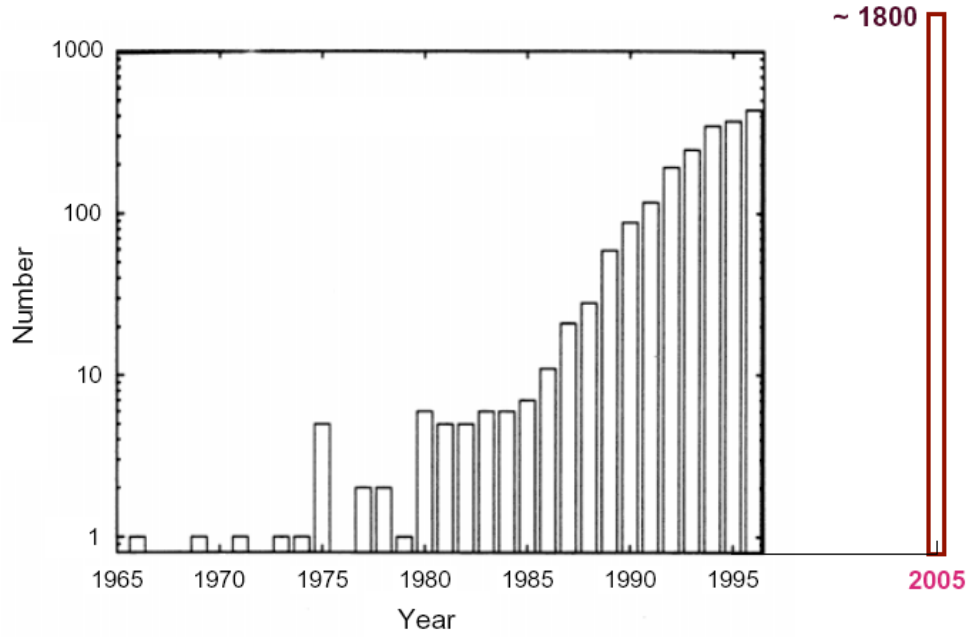

Fig. 1. Yearly FDTD-related publications. Data source for years 1966–96: Shlager and Schneider [2]. The 2005 data point is an estimate based upon a Web of Science® search by the author.

1054-4887 © 2007 ACES

II. HISTORY OF FDTD TECHNIQUES FOR MAXWELL'S EQUATIONS

We can begin to develop an appreciation of the basis, technical development, and possible future of FDTD numerical techniques for Maxwell's equations by first considering their history. Table 1 lists some of the key initial publications in this area, starting with Yee's seminal paper [1].

Table 1

Partial History of FDTD and Related Techniques

1966	Yee [1] introduced the basic FDTD space grid and time-stepping algorithm.
1975	Taflove and Brodwin reported the correct numerical stability criterion for Yee's algorithm [3]; sinusoidal steady-state Yee-based solutions of 2-D and 3-D electromagnetic wave interactions with material structures [3, 4]; and Yee-based bioelectromagnetics models [4].
1977	Holland [5] and Kunz and Lee [6] applied Yee's algorithm to EMP problems.
1977, 1980	Engquist and Majda [7] and Bayliss and Turkel [8] reported second-order accurate absorbing boundary conditions (ABCs) for grid-based time-domain wave-propagation schemes
1980	Taflove coined the FDTD acronym and published validated models of sinusoidal steady-state electromagnetic wave penetration into a 3-D metal cavity [9].
1981	Mur reported a second-order accurate ABC for Yee's grid [10] based upon the Engquist-Majda theory.
1982, 3	Taflove and Umashankar [11, 12] reported a phasor-domain near-to-far field transformation which permits calculating the far fields and radar cross-section of 2-D and 3-D structures.
1984	Liao et al. [13] reported a novel space-time extrapolation ABC that is less reflective than Mur's ABC.
1985	Gwarek introduced an lumped equivalent-circuit formulation [14].
1986	Choi and Hoefer modeled waveguide structures [15].
1987, 8	Kriegsmann et al. and Moore et al. published the first articles on ABC theory in *IEEE Trans. Antennas and Propagation* [16, 17].
1987, 8, 1992	Contour-path subcell techniques were introduced by Umashankar et al. to model thin wires and wire bundles [18]; by Taflove et al. to model penetration through cracks in metal screens [19]; and by Jurgens et al. to conformally model smoothly curved surfaces [20].
1987, 1990	Finite-element time-domain (FETD) and finite-volume time-domain (FVTD) meshes were introduced by Cangellaris et al. [21], Shankar et al. [22], and Madsen and Ziolkowski [23].
1988	Sullivan et al. published a 3-D model of sinusoidal steady-state electromagnetic wave absorption by a complete human body [24].
1988	Zhang et al. modeled microstrips [25].
1989	Fang [26] introduced higher-order spatial derivatives.
1990, 1	Kashiwa and Fukai [27], Luebbers et al. [28], and Joseph et al. [29] modeled frequency-dependent dielectric permittivity.
1990, 1	Maloney et al. [30], Katz et al. [31], and Tirkas and Balanis [32] modeled antennas.
1990	Sano and Shibata [33] and El-Ghazaly et al. [34] modeled picosecond optoelectronic switches.
1991	Luebbers et al. [35] introduced the time-domain near-to-far field transformation.
1991-4	Optical pulse propagation in nonlinear media was reported, including temporal solitons by Goorjian and Taflove [36]; beam self-focusing by Ziolkowski and Judkins [37]; and spatial solitons by Joseph and Taflove [38].
1991-8	Digital processing of windowed FDTD time-waveforms was introduced by several groups [39-43] to allow extracting the underlying resonant frequencies and quality factors.
1992	Sui et al. modeled lumped circuit elements [44].
1993	Toland et al. modeled tunnel diodes and Gunn diodes exciting cavities and antennas [45].
1994	Thomas et al. [46] reported SPICE subgrid models of embedded electronic components.
1994	Berenger introduced the extraordinarily effective perfectly matched layer (PML) ABC for 2-D grids [47], which was later extended to 3-D grids by Katz et al. [48] and to dispersive waveguide terminations by Reuter et al. [49].
1995, 6	Sacks et al. [50] and Gedney [51] introduced a physically realizable, uniaxial perfectly matched layer (UPML) ABC.

Table 1 (continued)

Partial History of FDTD Techniques for Maxwell's Equations

1995, 8 2002, 4	Hybrid FDTD-quantum mechanics models of two-level and four-level atoms were introduced by several groups [52-55] to model ultrafast optical interactions and lasing phenomena.
1996	Krumpholz and Katehi [56] introduced the multiresolution time-domain (MRTD) technique based upon wavelet expansion functions.
1996, 7	Liu [57, 58] introduced the pseudospectral time-domain (PSTD) method, which permits coarse spatial sampling approaching the Nyquist limit.
1997	Ramahi [59] introduced complementary operators method (COM) analytical ABCs.
1997	Dey and Mittra [60] introduced a simple, stable, accurate contour-path technique to model curved metal surfaces.
1998	Maloney and Kesler [61] introduced several novel means to analyze periodic structures.
1999	Schneider and Wagner [62] reported a rigorous analysis of grid dispersion.
1999, 2000	Namiki [63] and Zheng, Chen, and Zhang [64] introduced 3-D alternating-direction implicit (ADI) FDTD algorithms with provable unconditional numerical stability.
2000	Roden and Gedney introduced the convolutional PML (CPML) ABC [65].
2000	Rylander and Bondeson introduced a provably stable FDTD-FE hybrid technique [66].
2002-6	Hayakawa et al. [67] and Simpson and Taflove [68, 69] reported models of the entire Earth-ionosphere waveguide for extremely low-frequency geophysical phenomena.
2003	DeRaedt introduced the unconditionally stable, "one-step" FDTD technique [70].

III. TECHNOLOGY DEVELOPMENT THEMES

In addition to the chronological summary provided in Table 1, it is useful to organize the past 40 years of FDTD developments according to their primary technology-development themes. These are summarized in Table 2, referencing the key initial publications listed in Table 1.

Table 2

Primary FDTD Technology Development Themes

- Absorbing boundary conditions
  - Engquist-Majda one-way wave equation, 1977 [7]
  - Bayliss-Turkel outgoing wave annihilators, 1980 [8]
  - Liao et al. extrapolation of outgoing waves in space and time, 1984 [13]
  - Berenger perfectly matched layer, 1994 [47]
  - Uniaxial perfectly matched layer, 1995-6 [50, 51]
  - Roden and Gedney convolutional perfectly matched layer, 2000 [65]
- Digital signal processing
  - Umashankar and Taflove, phasor-domain near-to-far field transformation, 1982, 83 [11, 12]
  - Luebbers et al. time-domain near-to-far field transformation, 1991 [35]
  - Extraction of underlying resonant frequencies and quality factors from windowed FDTD time-waveforms 1991-8 [39-43].
- Numerical dispersion
  - Fang higher-order spatial derivatives, 1989 [26]
  - Krumpholz and Katehi MRTD, 1996 [56]
  - Q. H. Liu PSTD, 1996-7 [57, 58]
  - Schneider and Wagner analysis for Yee FDTD, 1999 [62]
- Numerical stability
  - Taflove and Brodwin analysis, 1975 [3]
  - Unconditionally stable ADI techniques, 1999-2000 [63, 64]
  - DeRaedt "one-step" FDTD technique, 2003 [70].
- Conforming grids
  - Locally conforming contour-path subcell techniques, 1987, 88, 92, 97 [18-20, 60]
  - Globally conforming grids, 1990 [22, 23]
  - Rylander and Bondeson stable hybrid FETD / FDTD, 2000 [66]

Table 2 (continued)

Primary FDTD Technology Development Themes

- Dispersive and nonlinear materials
  - — Linear dispersions, 1990,91 [27-29]
  - — Nonlinearities, yielding self-focusing and temporal and spatial solitons, 1991-4 [36-38]
- Multiphysics coupling to Maxwell's equations
  - – Charge generation, recombination, and transport in semiconductors, 1990 [33, 34]
  - – Electron transitions between multiple energy levels of atoms, modeling pumping, emission, and stimulated emission processes, 1995, 1998, 2002, 2004 [52-55]

IV. CURRENT AND EMERGING FDTD APPLICATIONS

This section illustrates current and emerging FDTD computational electrodynamics modeling applications over the frequency range from about 1 Hz to 6 $\times 10^{14}$ Hz (i.e., extremely low frequencies to daylight).

A. Extremely Low Frequency Models of the Earth-Ionosphere Waveguide

FDTD has been recently applied to model extremely low frequency (ELF) electromagnetic wave propagation within the Earth-ionosphere waveguide. Fig. 2 illustrates the most advanced gridding technique used in such studies, and sample results for antipodal wave propagation around the Earth calculated using a high-resolution grid with space cells spanning only about 40 km over the entire surface of the planet.

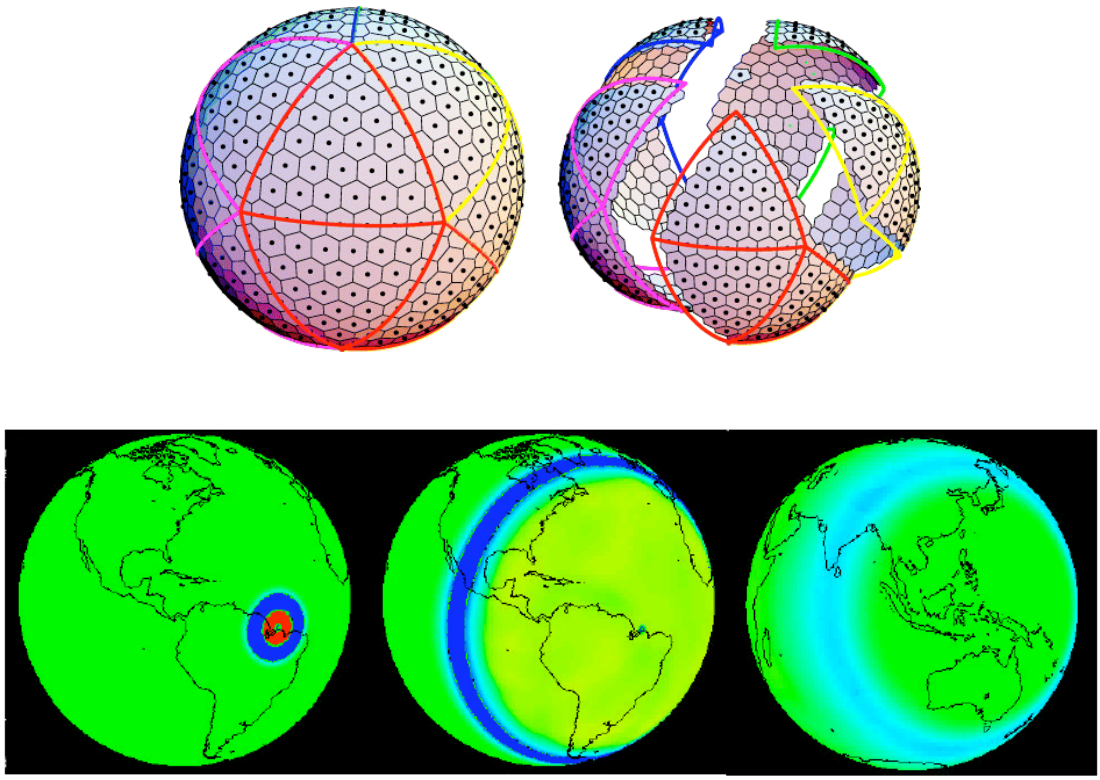

Fig. 2. FDTD model of the Earth-ionosphere waveguide. Top: geodesic grid [69]. Bottom: snapshots of impulsive wave propagation around the Earth (the complete video can be downloaded at `http://www.ece.northwestern.edu/ecefaculty/taflove/3Dmovietext@gif.avi`)

B. Wireless Personal Communications Devices

Figs. 3-5 illustrate how FDTD has been applied to provide accurate, high-resolution models of cellphones [71]. Here, the grid-cell size is as fine as 0.1 mm to resolve fine geometrical details.

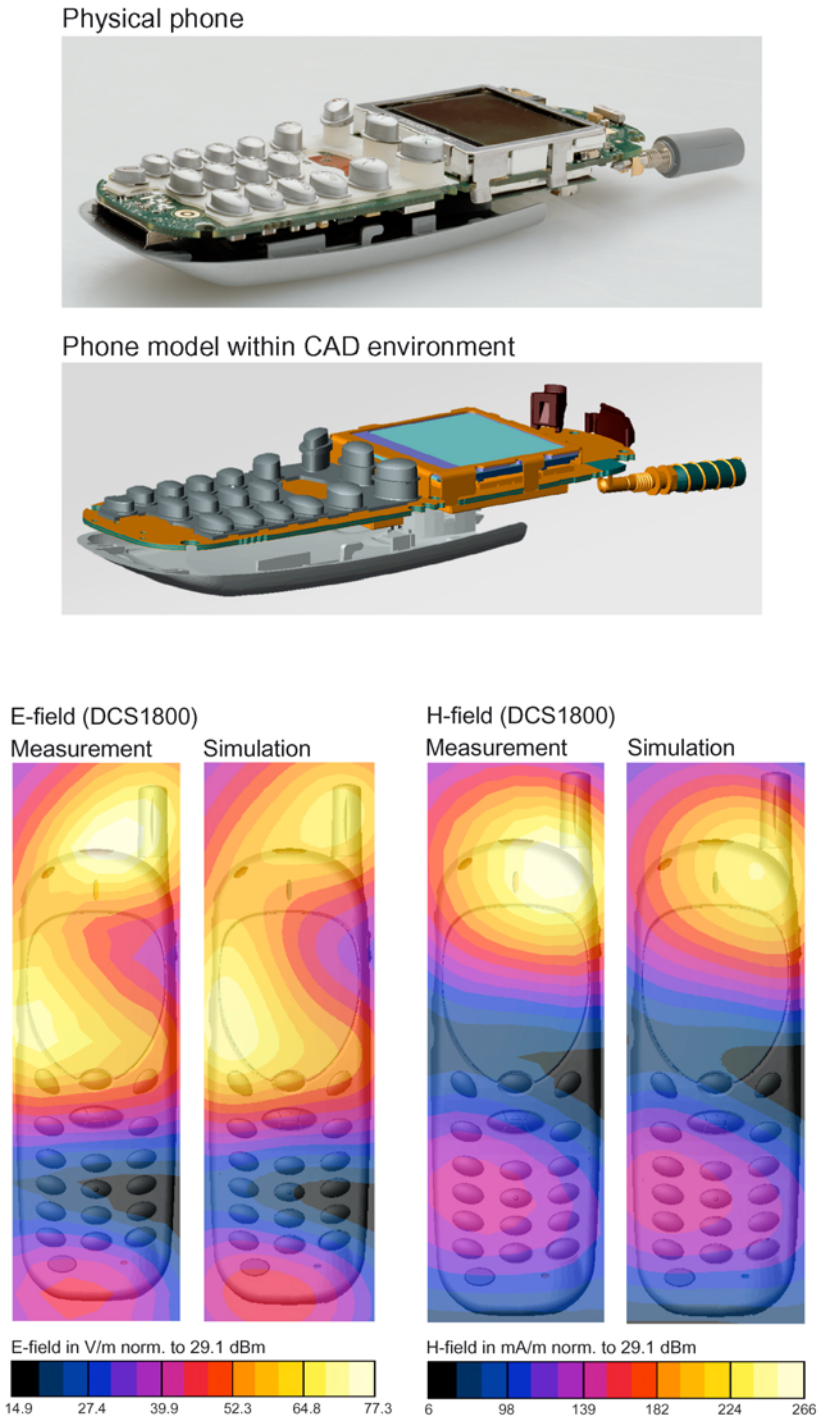

Fig. 3. FDTD model of the Motorola T250 cellphone [71]. Top: physical phone and the FDTD CAD model. Bottom: agreement of measured and FDTD-calculated near-surface electromagnetic fields at 1.8 GHz.

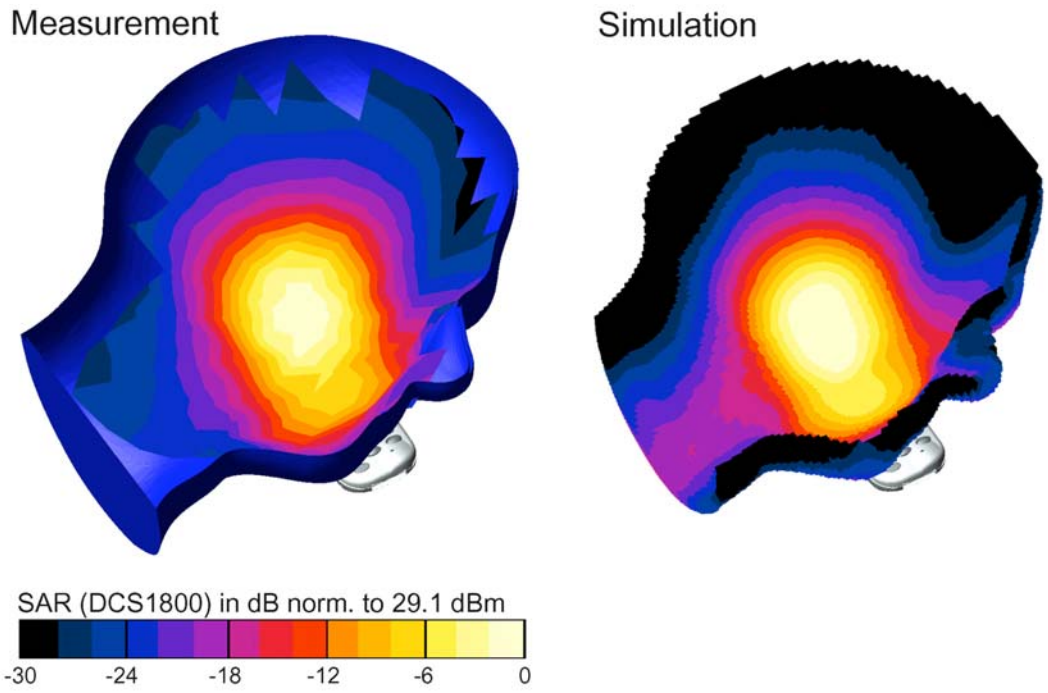

Fig. 4. Agreement of the measured and FDTD-calculated specific absorption rate (SAR) at 1.8 GHz for the cellphone of Fig. 3 positioned adjacent to a standard phantom head model [71].

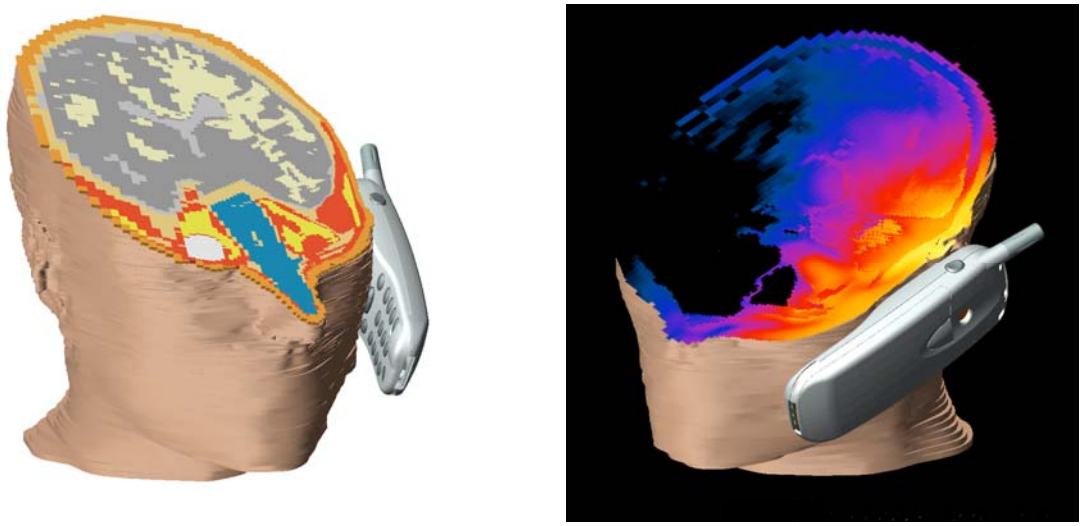

Fig. 5. FDTD-calculated SAR at 1.8 GHz for the cellphone of Fig. 3 positioned adjacent to a realistic head model derived from tomographic scans of a volunteer subject [71]. The head model has 121 slices (1 mm thick in the ear region, 3 mm thick elsewhere), wherein each slice has a transverse resolution of 0.2 mm.

C. Ultrawideband Microwave Detection of Early-Stage Breast Cancer

Fig. 6 illustrates how FDTD has been applied to model a proposed ultrawideband (UWB) microwave technique for early detection of breast cancer [72]. Here, FDTD was used to model the breast tissues and an antenna system consisting of impulsive sources and receptors located at the surface of the breast. In the case shown, a 2-mm diameter malignant tumor was assumed to be embedded 3 cm within a realistic breast model derived from tomographic scans of a volunteer subject. The impulsive excitation had spectral components primarily in the 1-10 GHz range. FDTD-calculated data for the backscattering response observed at the antenna was post-processed to derive the image shown. From Fig. 6, we see that the proposed UWB microwave technique yields a cancer signature which should be readily detectable, i.e., 15 dB to 30 dB stronger than the clutter due to the surrounding normal tissues. This is very encouraging, since a small malignancy of this type would almost certainly not be detectable using x-ray mammography.

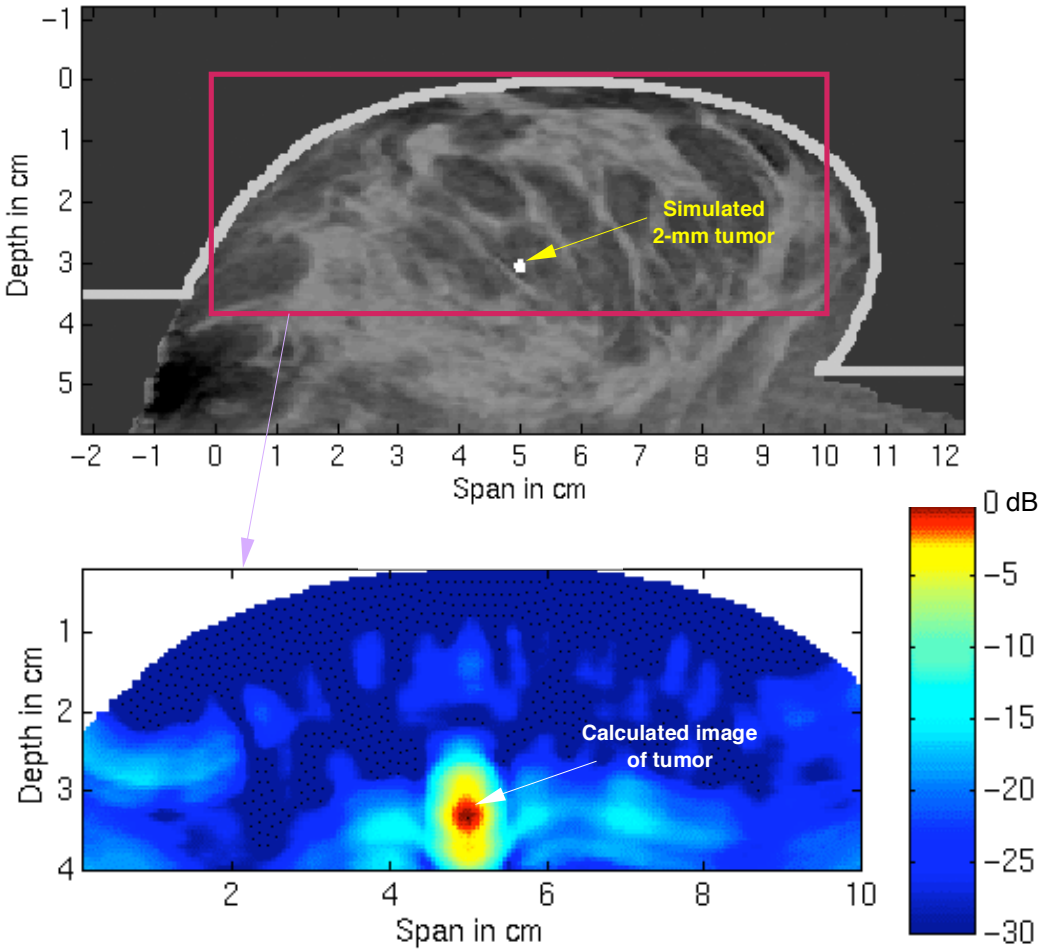

Fig. 6. Calculated image of a 2-mm diameter malignant tumor embedded 3 cm below the surface of a model of the female human breast [72]. This image was derived by post-processing FDTD data for the backscattering of ultrawideband electromagnetic wave pulses radiated by an antenna system located at the surface of the breast. The breast model was assembled from tomographic scans of a volunteer subject. The presence and location of the small tumor is easily discerned. Such a cancer would almost certainly not be detectable using x-ray mammography.

D. Ultrahigh-Speed Bandpass Digital Interconnects

Fig. 7 illustrates how FDTD has been applied to model proposed ultrahigh-speed substrate integrated waveguide (SIW) interconnects for digital circuits [73]. Each SIW would be implemented in a multilayer circuit board by inserting two parallel rows of vias to connect adjacent ground planes. With no center conductor required, high-characteristic-impedance operation is possible and copper losses can be significantly reduced relative to stripline interconnects. Furthermore, sharp bends up to 90˚ are possible with negligible reflections and little overall impact on the signal transmission. Fig. 7(top) is a photograph of a prototype straight SIW constructed and tested at Intel Corporation in summer 2005 [73]. Measurements confirmed the FDTD predictions (Fig. 7(bottom)) that both straight and bent SIWs exhibit 100% bandwidths with negligible multimoding, for this prototype, 27 GHz – 81 GHz. In ongoing work, half-width folded SIWs are predicted by FDTD to have even larger (115%) bandwidths. Board-level interconnects using this technology could stream digital data at rates 10 – 50 times greater than possible today, which would satisfy Intel's needs for the next decade.

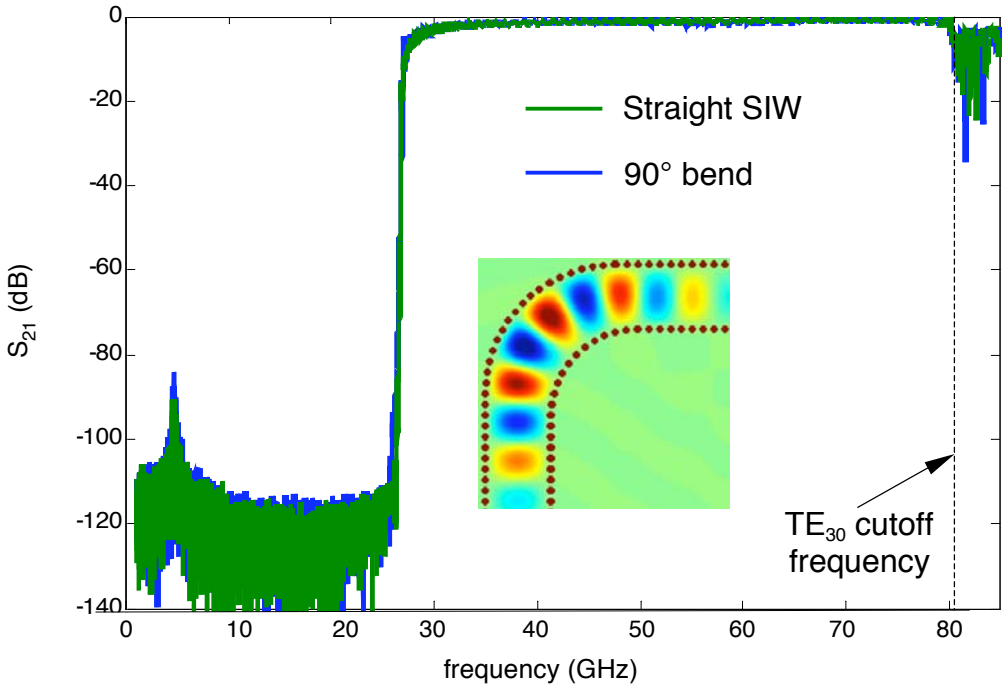

Fig. 7. FDTD-calculated S_{21} transmission versus frequency for the prototype substrate integrated waveguide board-level digital interconnect shown at the top [73]. FDTD predicts little difference in the S_{21} characteristic over the entire 100% bandwidth if a 90˚ bend is inserted (see inset for a snapshot visualization of the electric field within the bend, showing a clean pattern with no multimoding).

E. Micron/Nanometer Scale Photonic Devices: Category 1 (Linear)

Currently, FDTD is routinely applied by the photonics community to analyze and design micron- and nanometer-scale devices operating at infrared through visible-light wavelengths. Fig. 8 illustrates one recent application of 3-D linear FDTD modeling to design a microcavity laser [74]. This electrically driven, single-mode device employs a photonic bandgap defect-mode cavity and operates at room temperature with a low threshold current. The physics of electromagnetic wave confinement by the cavity is properly simulated.

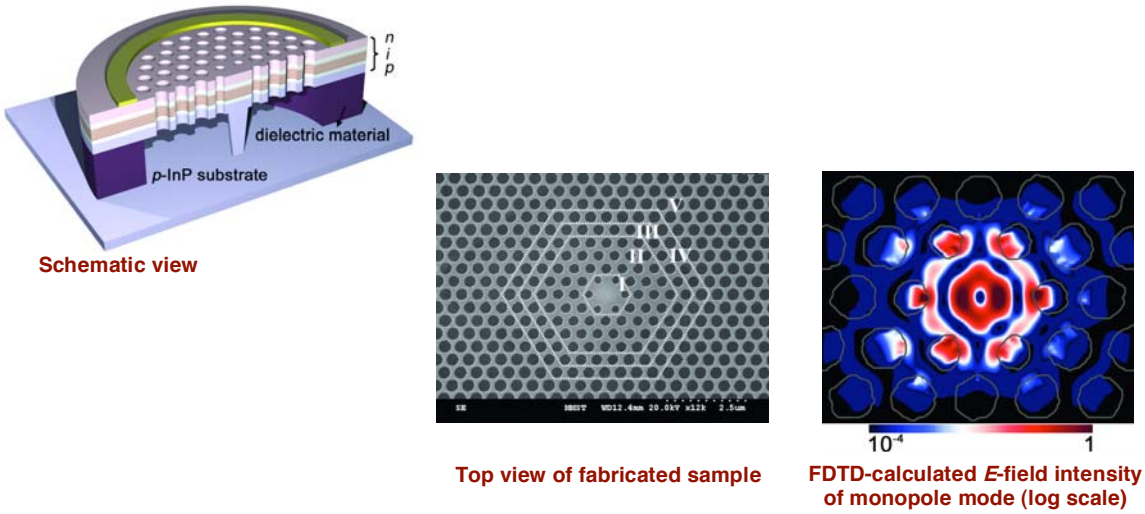

Fig. 8. Application of 3-D FDTD modeling to design a photonic bandgap defect-mode microcavity laser [74].

Fig. 9 illustrates a recent application of 3-D linear FDTD modeling to analyze the transmission of 532-nm wavelength light through a 200-nm diameter hole in a 100-nm thick gold film [75]. This illustrates the capability of a dispersive FDTD algorithm to properly model the formation of a plasmon mode at the surface of the gold film, which enhances the transmission of the normally incident light through the small hole.

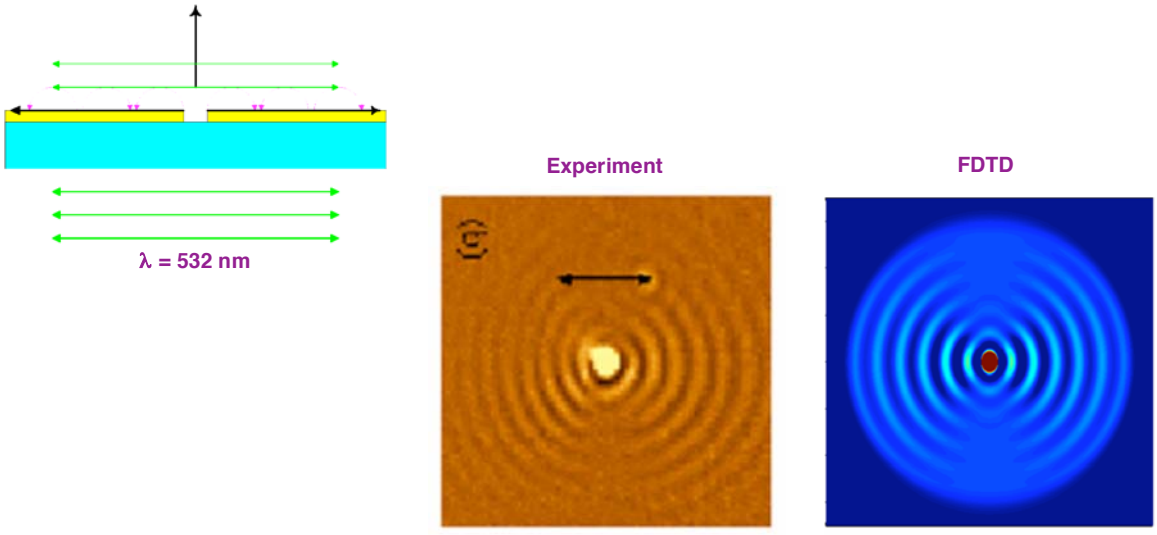

Fig. 9. Application of 3-D FDTD modeling to analyze enhanced light transmission through a sub-micron hole in a gold film due to the formation of a plasmon mode at the surface of the film [75].

F. Micron/Nanometer Scale Photonic Devices: Category 2 (Macroscopic Nonlinearity and Gain)

The incorporation of material nonlinearity and gain is an emerging area in FDTD modeling of micron- and nanometer-scale photonic devices. One approach incorporates nonlinearity and/or gain in the macroscopic description of the dielectric polarization or the index of refraction. Such nonlinearity and gain can be either independent or dependent upon the optical wavelength. Fig. 10 illustrates the first reported application of nonlinear FDTD modeling to simulate the propagation and interaction of spatial optical solitons [38]. Here, parallel, co-propagating, equal-amplitude spatial solitons having a dielectric wavelength of 528 nm in a glass medium exhibit a periodic coalescence or "braiding" if the optical carriers are assumed to be in phase. If the optical carriers are assigned a relative phase of π, FDTD modeling shows that the spatial solitons either immediately diverge to infinite separation or coalesce once before diverging. Such phenomena can form the basis of an ultrafast all-optical switch.

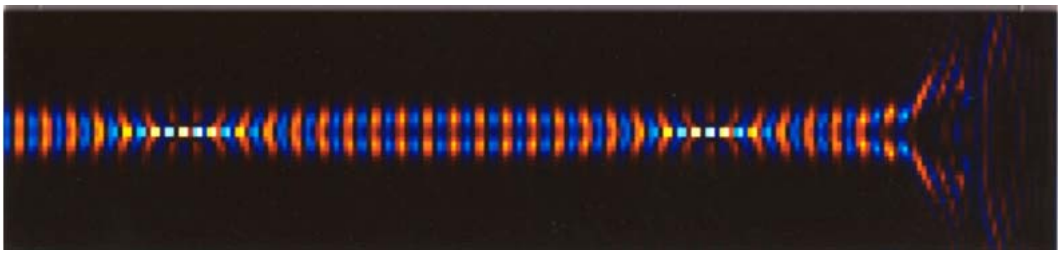

Fig. 10. Application of 2-D nonlinear FDTD modeling to analyze the periodic "braiding" of co-phased spatial optical solitons in glass [38]. The solitons propagate from left to right.

Fig. 11 illustrates an interesting recent application of 2-D nonlinear FDTD modeling to analyze the operation of a proposed low-power all-optical switch implemented in the crossing junction of photonic crystal defect-mode waveguides [76]. Here, the control signal perturbs the refractive index (and thereby the resonant frequency) of a defect-mode cavity at the intersection of the waveguides. This flips the cavity's transmission of the signal from stopband to passband, permitting the signal to reach the output port.

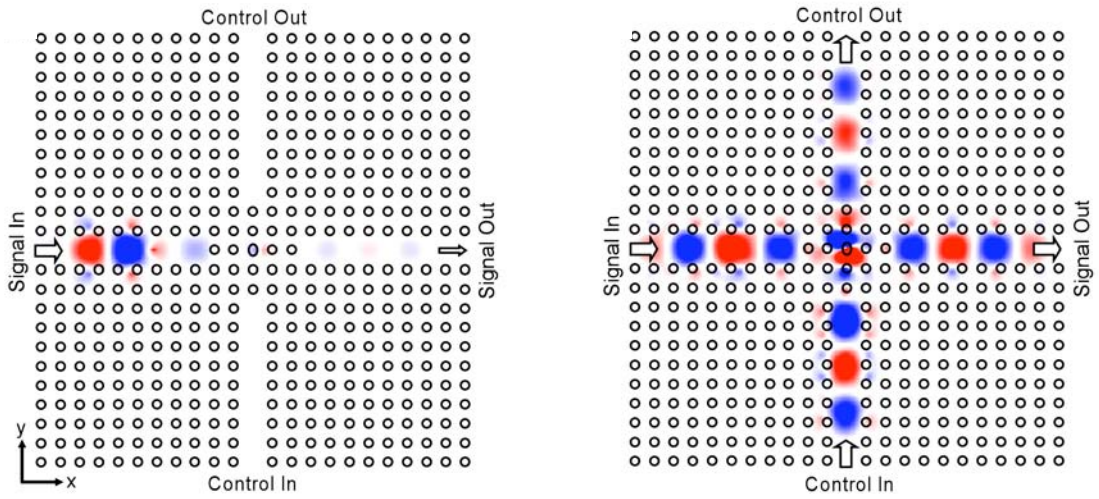

(a) control input is absent, yielding low signal output (b) control input is present, yielding high signal output

Fig. 11. Application of 2-D nonlinear FDTD modeling to analyze a proposed all-optical switch [76].

G. Micron/Nanometer Scale Photonic Devices: Category 3 (Semiclassical Models)

A second, more rigorous and more flexible approach to incorporate nonlinearity and gain in optical media involves time-stepping concurrently with the normal FDTD field updates a set of auxiliary differential equations which describes the behavior of individual atoms and their electrons. Phenomena of interest here include electron transitions between multiple energy levels of atoms that involve pumping, emission, and stimulated emission processes [52-55]. With this technique, quantum phenomena are coupled to the classical Maxwell's equations, yielding what may be called a semiclassical model.

Fig. 12 illustrates recent modeling results for electron population inversion and lasing output vs. time obtained using the semiclassical four-level-atom FDTD model reported in [55]. This laser is assumed to have a one-dimensional, optically pumped, single-defect, distributed Bragg reflector cavity with three layers of refractive indices alternating between n = 1.0 and 2.0, with thickness 375 nm and 187.5 nm, respectively.

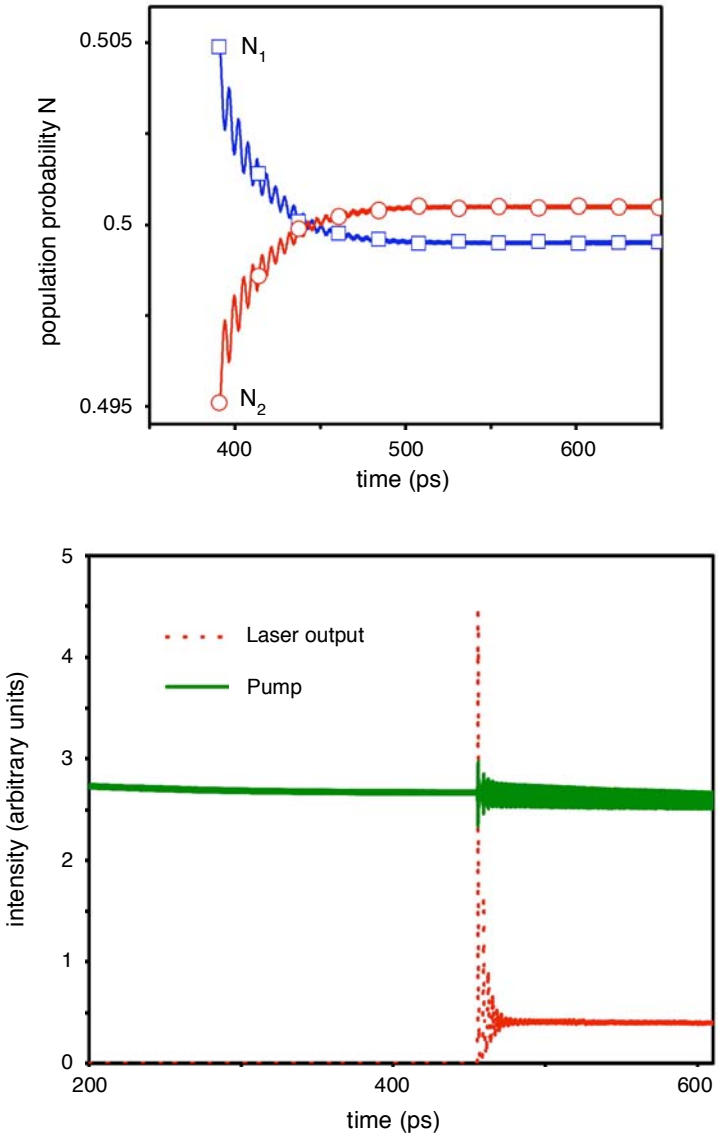

Fig. 12. Top: electron population density probability showing the inversion between Levels 1 and 2; Bottom: intensity output of the pump and laser output signals [55].

H. Biophotonics: Category 1 (Optical Interactions with Small Numbers of Living Cells)

Another important emerging application for FDTD modeling involves analyzing optical scattering by human biological cells and tissues. Such analyses are currently playing a key role in developing novel medical techniques for detecting precancerous conditions in the cervix and colon, with potential additional early detection applications for pancreatic, esophageal, and lung cancers. Fig. 13 illustrates the goal: to unambiguously distinguish normal cells from distressed cells when conventional optical microscopy fails.

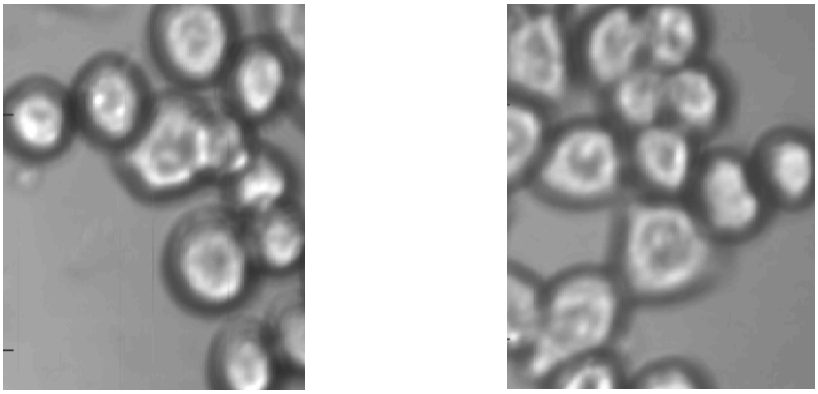

(a) Normal cells (b) Distressed chemically treated cells

Fig. 13. Similar conventional microscope images: (a) normal HT-29 cells; (b) distressed chemically treated cells.

Fig. 14 illustrates applying FDTD to evaluate the sensitivity of optical backscattering and forward-scattering to small, random, refractive-index fluctuations spanning nanometer length scales [77]. Here, the spectral / angular distribution of scattered light from a randomly (and weakly) inhomogeneous dielectric sphere is compared to that for the homogeneous sphere of the same size and average refractive index.

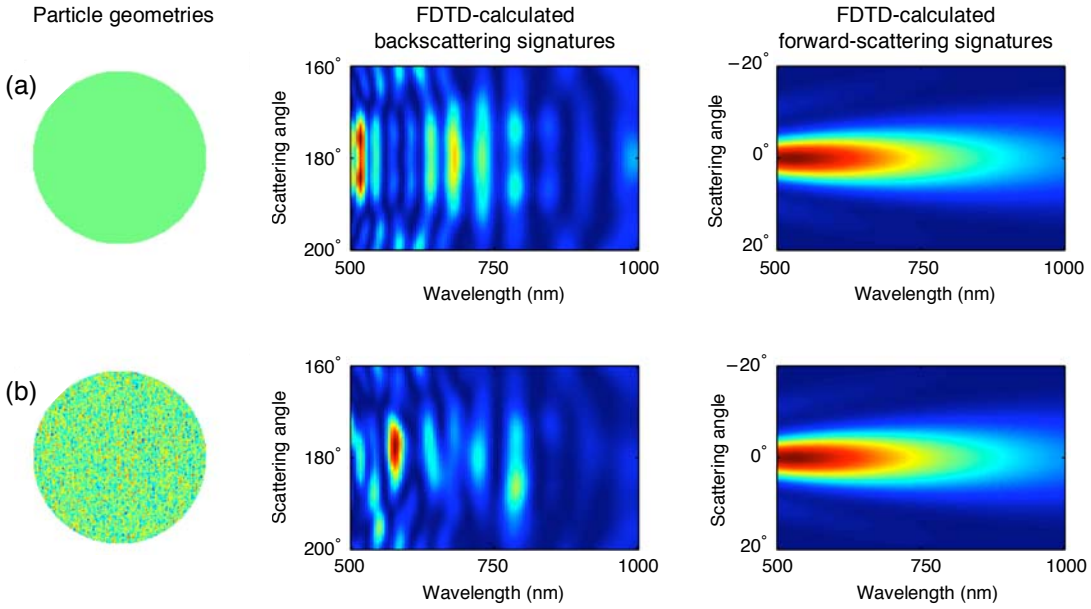

Fig. 14. FDTD-computed optical scattering signatures of a 4-μm-diameter sphere with average refractive index n_{avg} = 1.1: (a) homogeneous sphere; (b) random index fluctuations (Δn = ±0.03; ~50 nm) within sphere.

From Fig. 14, we see that that there exists distinctive features of the backscattering spectral / angular distribution for the inhomogeneous case of Fig. 14(b) despite the fact that the inhomogeneities for this case are weak (only 3%) and much smaller (only about 50 nm) than the diffraction limit at the illuminating wavelengths. In contrast, the forward-scattering signature in Fig. 14(b) exhibits no distinctive features.

These FDTD models have supported laboratory optical backscattering measurements of rat colon tissues treated with the carcinogen AOM [78]. As shown in Fig. 15, only two weeks after application of the AOM, the treated colon tissues exhibited perturbed backscattering spectra apparently caused by the formation of subdiffraction tissue inhomogeneities akin to those in Fig. 14(b). Note that these could *not* be seen under a microscope. In fact, *these precancerous changes could not be detected by any existing pathology technique.* These findings led to the development of a preclinical instrument which has shown excellent sensitivity and specificity in initial trials with several hundred human subjects [79]. Currently, these trials are being greatly expanded.

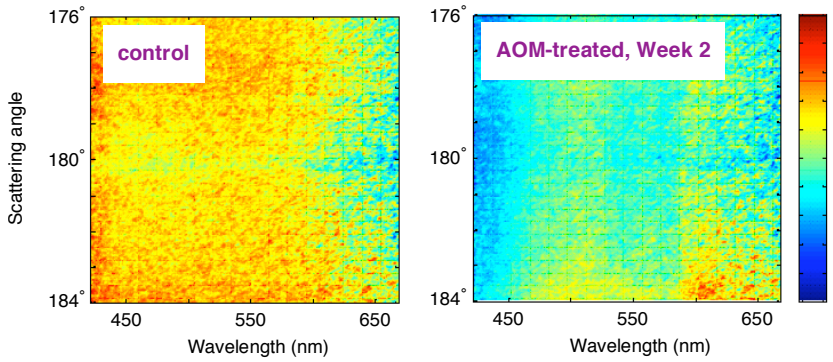

Fig. 15. Typical measured backscattering spectral / angular distributions for rat colon tissues [78].

Current FDTD modeling work in this area has shifted toward spectral analysis of individual backscattered pixels so that highly localized changes *within a single biological cell* can be investigated. First, as illustrated in Fig. 16, the near-to-far field transformation was augmented to yield a backscattered amplitude *image* [80].

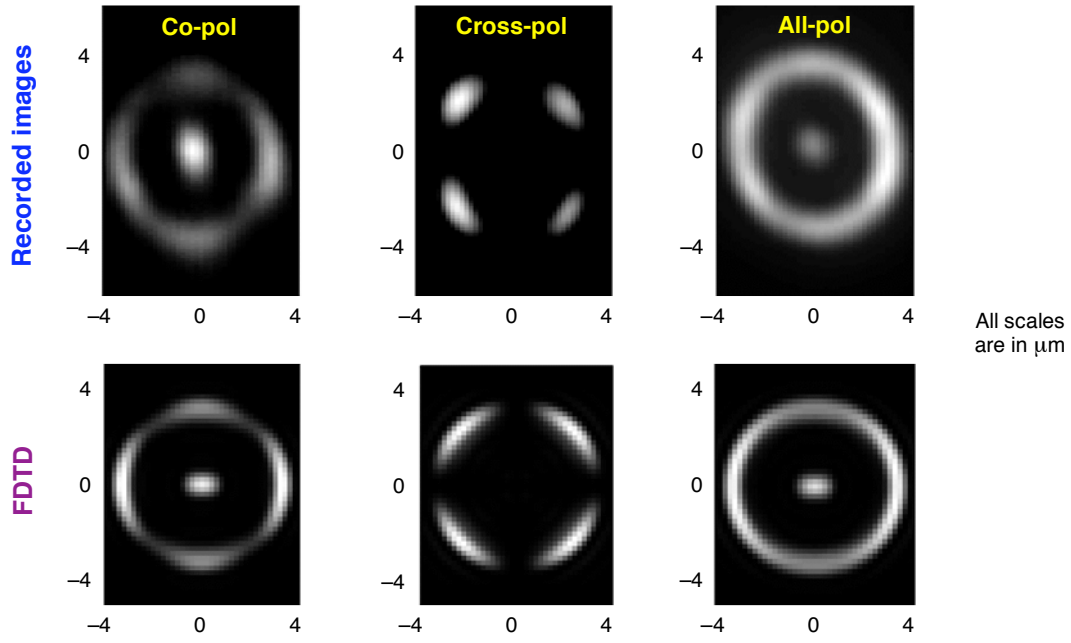

Fig.16. Agreement of measured / FDTD-calculated backscattered amplitude images of 6-μm dielectric sphere [80].

Next, assuming a normally incident plane wave, FDTD was used to calculate the optical spectra of individual pixels within the backscattered amplitude image of a rectangular layered material slab. Referring to Fig. 17, each layer of the slab was assumed to have a thickness in the order of 25 nanometers, with sub-micron lateral "checkerboard" inhomogeneities near the diffraction limit. As shown in this figure, it was determined that the backscattered spectra at pixels centered within each checkerboard square were highly correlated with those for a material slab having the same nanometer-scale layering, but no lateral variations (i.e., a 1-D illumination geometry) [81]. This yields additional evidence that nanometer-scale inhomogeneities can cause pronounced alterations of backscattering spectra. Furthermore, it suggests means to deduce the local layering of an inhomogeneous material structure (such as a living cell) by analyzing the spectra of individual pixels within its backscattered amplitude image.

Finally, exploiting the insights developed via FDTD modeling, a microscope system was constructed to acquire pixel-by-pixel backscattering spectra of individual living cells [81]. As shown in Fig. 18, this system was readily able to distinguish the normal HT-29 cells of Fig. 13 from their distressed, chemically treated counterparts.

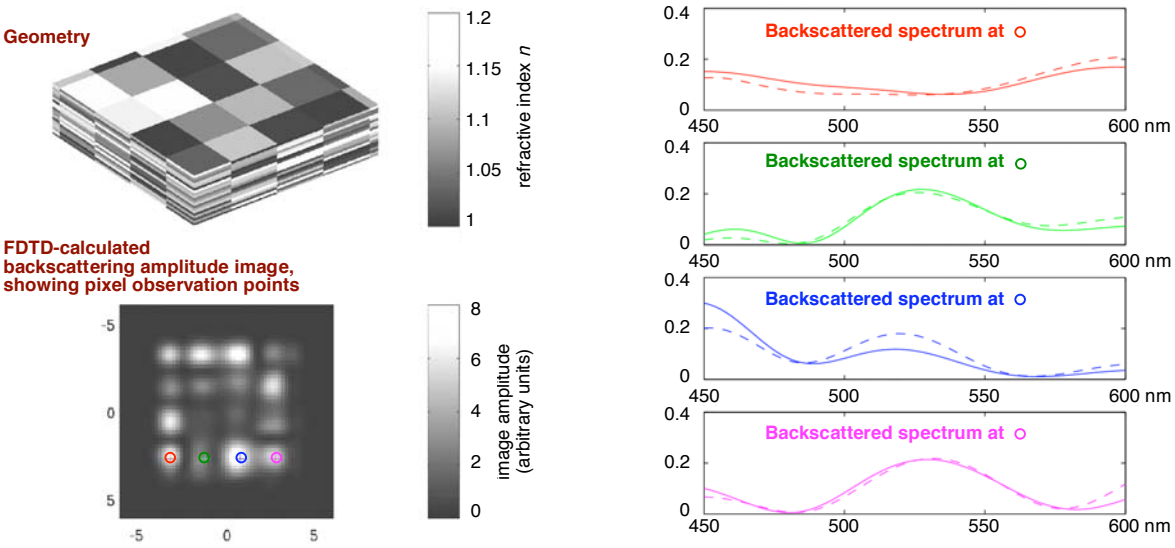

Fig. 17. FDTD-calculated spectra of four distinct pixels within the backscattered amplitude image of a layered material slab [81].

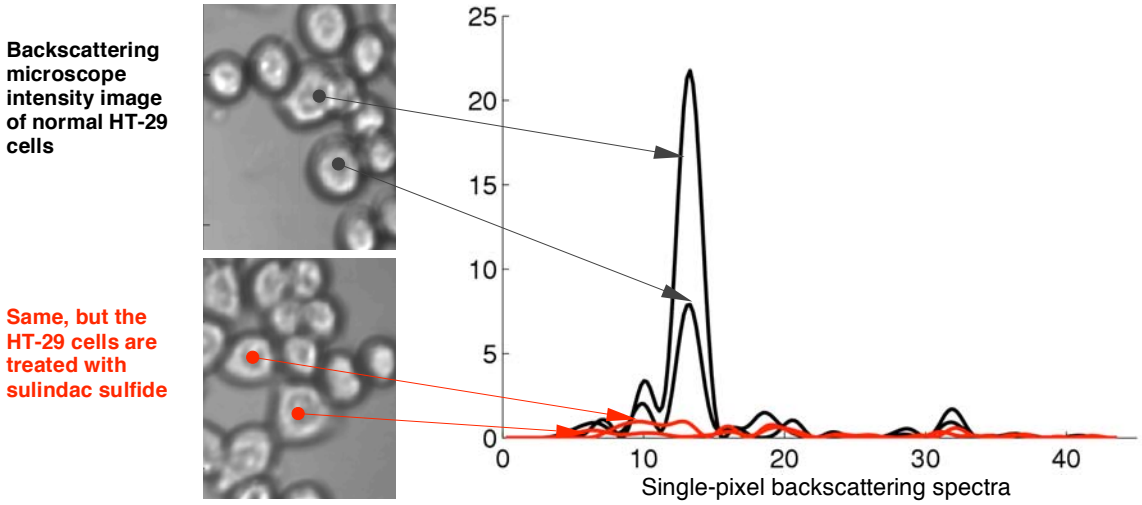

Fig. 18. Normal HT-29 cells have different pixel backscattering spectra than those chemically treated [81].

I. Biophotonics: Category 2 (Optical Interactions with Large Numbers of Living Cells)

Pseudospectral time-domain (PSTD) computational solutions of Maxwell's equations introduced by Liu [57, 58] permit coarse spatial sampling approaching the Nyquist limit. This characteristic of PSTD techniques permits modeling electromagnetic wave interactions in 3-D spatial regions spanning many tens of wavelengths. As a consequence, an important emerging biophotonics application of PSTD modeling involves analyzing light propagation through, and scattering by, large clusters of living cells; in fact, much larger clusters than possible using traditional FDTD techniques. Obtained directly from Maxwell's equations, PSTD solutions are more rigorous than many approximate techniques that are widely used by the biophotonics community. Hence, PSTD modeling affords new opportunities to advance a wide range of medical diagnoses and treatments that are based upon interactions of light with biological tissues.

Fig. 19 illustrates the accuracy of the Fourier-basis 3-D PSTD technique in calculating the differential scattering cross-section of a single dielectric sphere (diameter d = 8 μm, refractive index n = 1.2) [82]. The PSTD solution (wavelength λ_0 = 750 nm, grid resolution Δ = 83.3 nm, staircased surface) agrees very well with the Mie series over a range of about 10^5:1. Fig. 20 illustrates the accuracy of this technique in calculating the total scattering cross-section (TSCS) of a 20-μm cluster of 19 randomly positioned dielectric spheres (each d = 6 μm, n = 1.2) [82]. Here, the PSTD solution (Δ = 167 nm, staircased surfaces) agrees well with the results of a multi-sphere series expansion.

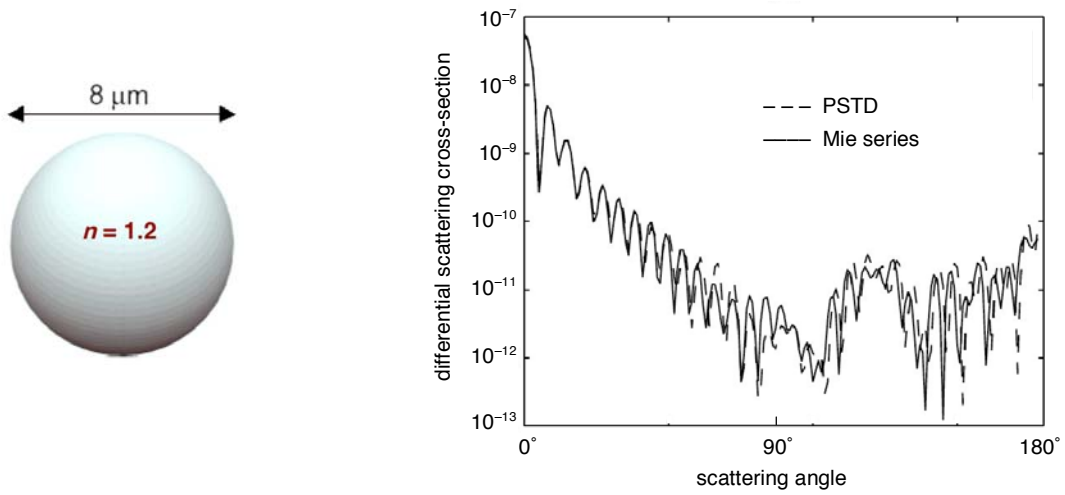

Fig. 19. Validation of Fourier-basis PSTD for scattering by a single sphere [82].

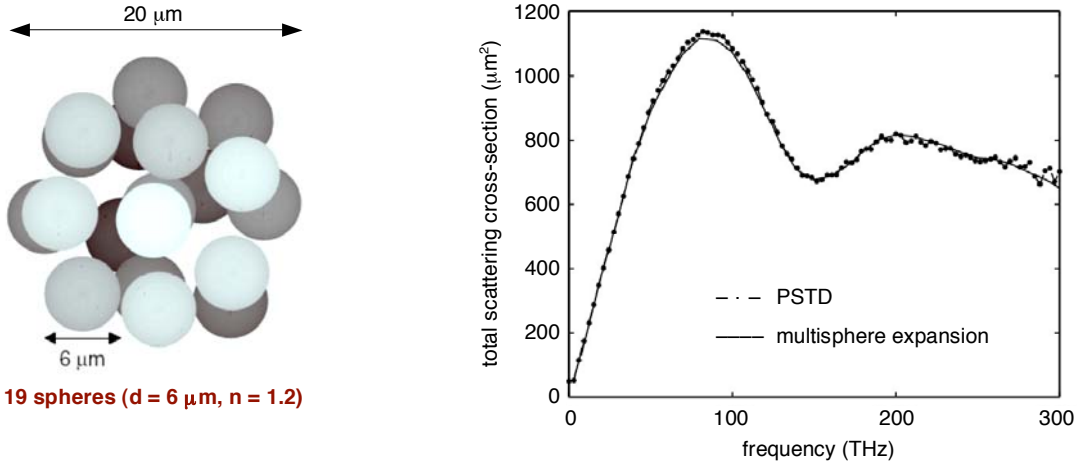

Fig. 20. Validation of Fourier-basis PSTD for scattering by a 20-μm cluster of 19 dielectric spheres [82].

The capability of the Fourier-basis 3-D PSTD technique to accurately solve the full-vector Maxwell's equations for closely coupled, electrically large objects opens up possibilities for accurately modeling optical interactions with clusters of biological cells. Fig. 21 illustrates a generic example wherein information regarding the diameter of individual particles within a cluster is obtained from its PSTD-computed TSCS [82]. Fig. 21(top) graphs versus frequency the PSTD results (grid resolution Δ = 167 nm, staircased surfaces) for the TSCS of a 25-μm cluster of 192 randomly positioned dielectric spheres (each d = 3 μm, n = 1.2). Now, we perform a cross-correlation of this data set with the TSCS-versus-frequency characteristic of a single "trial" dielectric sphere of refractive index n = 1.2 and adjustable diameter d. We hypothesize that the maximum cross-correlation is achieved when the diameter of the trial sphere equals the diameter of the individual spheres comprising the cluster. Indeed, Fig. 21(bottom) shows that the peak cross-correlation occurs when the diameter of the trial sphere is 3.25 μm, within 10% of the actual 3 μm diameter. Similar results have been reported for a variety of clusters of dielectric spheres [82].

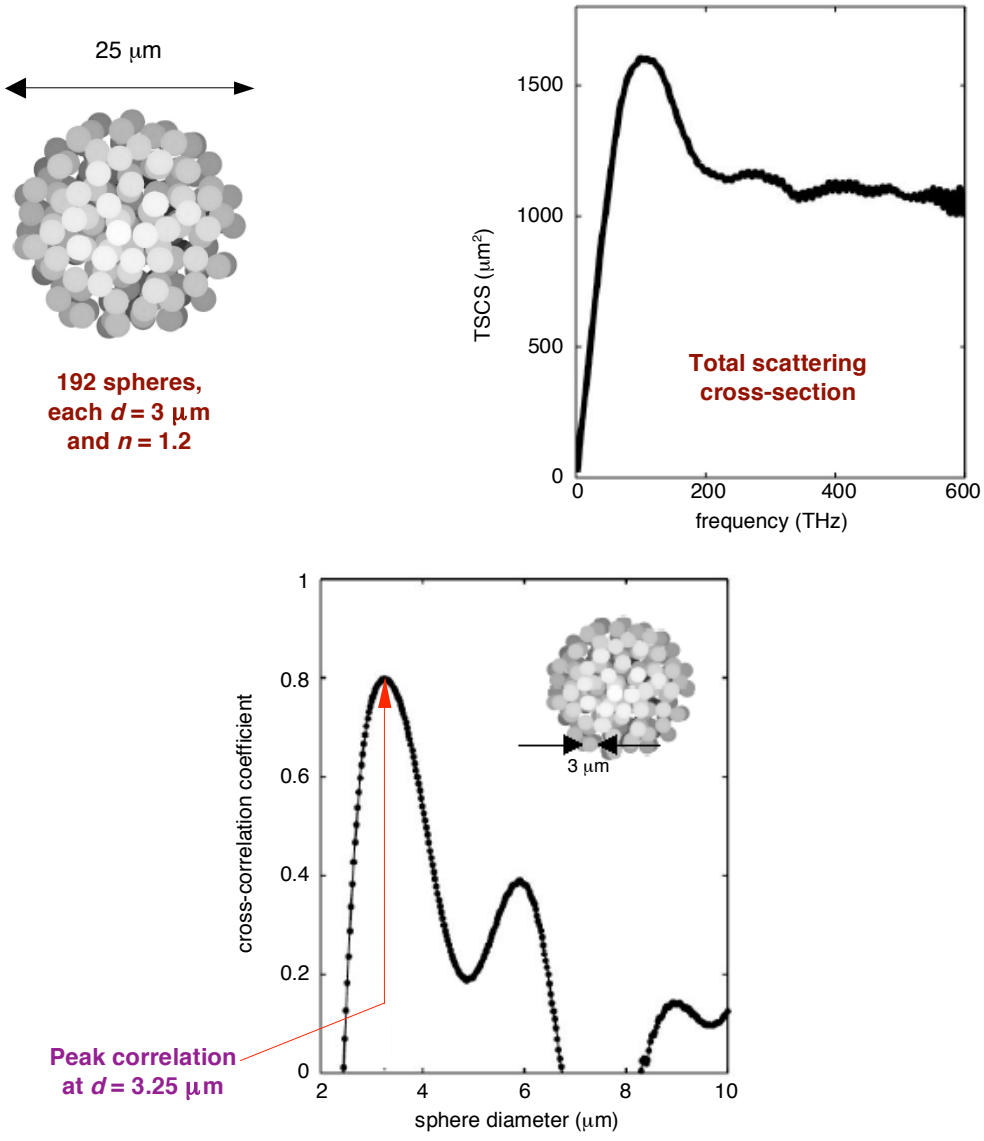

Fig. 21. Top: PSTD-calculated TSCS vs. frequency of a 25-μm cluster of 192 dielectric spheres (d = 3 μm, n = 1.2). Bottom: Cross-correlation of the top TSCS data set with the TSCS-vs.-frequency characteristic of a single trial dielectric sphere of the same refractive index (n = 1.2) but adjustable diameter [82].

V. FUTURE PROSPECTS

During the past 40 years since Yee's Paper #1, advances in FDTD theory and software and in general computing technology have elevated FDTD techniques to the top rank of computational tools for engineers and scientists studying electrodynamic phenomena and systems. There is every reason to believe that the steady pace of these advances will continue.

In particular, the author believes that a large expansion of FDTD and related techniques will occur in four research areas which cover the frequency spectrum from ELF past visible light: (1) geophysics and related remote sensing of the Earth and its atmosphere; (2) biophotonics; (3) nanometer-scale physics, especially interfacing with quantum electrodynamics; and (4) inverse scattering. Impacting these disparate areas is made possible by the extraordinary flexibility and robustness of FDTD and related grid-based time-domain solutions of Maxwell's equations, which arguably involve computational techniques which are the closest to how Mother Nature "solves" *her* electrodynamics problems.

ACKNOWLEDGEMENTS

The author recognizes the marvelous collaboration and warm friendship provided by Prof. Korada Umashankar during his all-too-brief lifetime. The author also says a hearty "thanks!" to all of his undergraduate and graduate research students over the years; to his project sponsors; and to his current collaborators, Profs. Vadim Backman and Xu Li of Northwestern University.

REFERENCES

[1] K. S. Yee, "Numerical solution of initial boundary value problems involving Maxwell's equations in isotropic media," *IEEE Trans. Antennas Propagat.*, vol. 14, pp. 302–307, 1966.

[2] K. L. Shlager and J. B. Schneider, "A Survey of the Finite-Difference Time-Domain Literature," Chap. 1 in *Advances in Computational Electrodynamics: The Finite-Difference Time-Domain Method*, A. Taflove, ed., Norwood, MA: Artech House, 1998.

[3] A. Taflove and M. E. Brodwin, "Numerical solution of steady-state electromagnetic scattering problems using the time-dependent Maxwell's equations," *IEEE Trans. Microwave Theory Tech.*, vol. 23, pp. 623–630, 1975.

[4] A. Taflove and M. E. Brodwin, "Computation of the electromagnetic fields and induced temperatures within a model of the microwave-irradiated human eye," *IEEE Trans. Microwave Theory Tech.*, vol. 23, pp. 888–896, 1975.

[5] R. Holland, "Threde: a free-field EMP coupling and scattering code," *IEEE Trans. Nuclear Sci.*, vol. 24, pp. 2416–2421, 1977.

[6] K. S. Kunz and K. M. Lee, "A three-dimensional finite-difference solution of the external response of an aircraft to a complex transient EM environment I: The method and its implementation," *IEEE Trans. Electromagn. Compat.*, vol. 20, pp. 328–333, 1978.

[7] B. Engquist and A. Majda, "Absorbing boundary conditions for the numerical simulation of waves," *Mathematics of Computation*, vol. 31, pp. 629–651, 1977.

[8] A. Bayliss and E. Turkel, "Radiation boundary conditions for wave-like equations," *Comm. Pure Appl. Math*., vol. 23, pp. 707–725, 1980.

[9] A. Taflove, "Application of the finite-difference time-domain method to sinusoidal steady-state electromagnetic penetration problems," *IEEE Trans. Electromagn. Compat.*, vol. 22, pp. 191–202, 1980.

[10] G. Mur, "Absorbing boundary conditions for the finite-difference approximation of the time-domain electromagnetic field equations," *IEEE Trans. Electromagn. Compat.*, vol. 23, pp. 377–382, 1981.

[11] K. R. Umashankar and A. Taflove, "A novel method to analyze electromagnetic scattering of complex objects," *IEEE Trans. Electromagn. Compat.*, vol. 24, pp. 397–405, 1982.

[12] A. Taflove and K. R. Umashankar, "Radar cross section of general three-dimensional scatterers," *IEEE Trans. Electromagn. Compat.*, vol. 25, pp. 433–440, 1983.

[13] Z. P. Liao, H. L. Wong, B. P. Yang, and Y. F. Yuan, "A transmitting boundary for transient wave analyses," *Scientia Sinica* (series A), vol. XXVII, pp. 1063–1076, 1984.

[14] W. Gwarek, "Analysis of an arbitrarily shaped planar circuit — A time-domain approach," *IEEE Trans. Microwave Theory Tech.*, vol. 33, pp. 1067–1072, 1985.

[15] D. H. Choi and W. J. Hoefer, "The finite-difference time-domain method and its application to eigenvalue problems," *IEEE Trans. Microwave Theory Tech*., vol. 34, pp. 1464–1470, 1986.

[16] G. A. Kriegsmann, A. Taflove, and K. R. Umashankar, "A new formulation of electromagnetic wave scattering using an on-surface radiation boundary condition approach," *IEEE Trans. Antennas Propagat.*, vol. 35, pp. 153–161, 1987.

[17] T. G. Moore, J. G. Blaschak, A. Taflove, and G. A. Kriegsmann, "Theory and application of radiation boundary operators," *IEEE Trans. Antennas Propagat.*, vol. 36, pp. 1797–1812, 1988.

[18] K. R. Umashankar, A. Taflove, and B. Beker, "Calculation and experimental validation of induced currents on coupled wires in an arbitrary shaped cavity," *IEEE Trans. Antennas Propagat.*, vol. 35, pp. 1248–1257, 1987.

[19] A. Taflove, K. R. Umashankar, B. Beker, F. A. Harfoush, and K. S. Yee, "Detailed FDTD analysis of electromagnetic fields penetrating narrow slots and lapped joints in thick conducting screens," *IEEE Trans*. *Antennas Propagat.*, vol. 36, pp. 247–257, 1988.

[20] T. G. Jurgens, A. Taflove, K. R. Umashankar, and T. G. Moore, "Finite-difference time-domain modeling of curved surfaces," *IEEE Trans. Antennas Propagat.*, vol. 40, pp. 357–366, 1992.

[21] A. C. Cangellaris, C.-C. Lin, and K. K. Mei, "Point-matched time-domain finite element methods for electromagnetic radiation and scattering," *IEEE Trans. Antennas Propagat.*, vol. 35, pp. 1160–1173, 1987.

[22] V. Shankar, A. H. Mohammadian, and W. F. Hall, "A time-domain finite-volume treatment for the Maxwell equations," *Electromagnetics*, vol. 10, pp. 127–145, 1990.

[23] N. K. Madsen and R. W. Ziolkowski, "A three-dimensional modified finite volume technique for Maxwell's equations," *Electromagnetics*, vol. 10, pp. 147–161, 1990.

[24] D. M. Sullivan, O. P. Gandhi, and A. Taflove, "Use of the finite-difference time-domain method in calculating EM absorption in man models," *IEEE Trans. Biomed. Engrg.*, vol. 35, pp. 179–186, 1988.

[25] X. Zhang, J. Fang, K. K. Mei, and Y. Liu, "Calculation of the dispersive characteristics of microstrips by the time-domain finite-difference method," *IEEE Trans. Microwave Theory Tech.*, vol. 36, pp. 263–267, 1988.

[26] J. Fang, *Time-Domain Finite Difference Computations for Maxwell's Equations*, Ph.D. dissertation, EECS Dept., Univ. of California, Berkeley, CA, 1989.

[27] T. Kashiwa and I. Fukai, "A treatment by FDTD method of dispersive characteristics associated with electronic polarization," *Microwave Optics Tech. Lett.*, vol. 3, pp. 203–205, 1990.

[28] R. Luebbers, F. Hunsberger, K. Kunz, R. Standler, and M. Schneider, "A frequency-dependent finite-difference time-domain formulation for dispersive materials," *IEEE Trans. Electromagn. Compat.*, vol. 32, pp. 222–229, 1990.

[29] R. M. Joseph, S. C. Hagness, and A. Taflove, "Direct time integration of Maxwell's equations in linear dispersive media with absorption for scattering and propagation of femtosecond electromagnetic pulses," *Optics Lett.*, vol. 16, pp. 1412–1414, 1991.

[30] J. G. Maloney, G. S. Smith, and W. R. Scott, Jr., "Accurate computation of the radiation from simple antennas using the finite-difference time-domain method," *IEEE Trans. Antennas Propagat.*, vol. 38, pp. 1059–1065, 1990.

[31] D. S. Katz, A. Taflove, M. J. Piket-May, and K. R. Umashankar, "FDTD analysis of electromagnetic wave radiation from systems containing horn antennas," *IEEE Trans. Antennas Propagat.*, vol. 39, pp. 1203–1212, 1991.

[32] P. A. Tirkas and C. A. Balanis, "Finite-difference time-domain technique for radiation by horn antennas," *Proc. 1991 IEEE Antennas Propagat. Soc. Intl. Symp.*, vol. 3, pp. 1750–1753, 1991.

[33] E. Sano and T. Shibata, "Fullwave analysis of picosecond photoconductive switches," *IEEE J. Quantum Electron.*, vol. 26, pp. 372–377, 1990.

[34] S. M. El-Ghazaly, R. P. Joshi, and R. O. Grondin, "Electromagnetic and transport considerations in subpicosecond photo-conductive switch modeling," *IEEE Trans. Microwave Theory Tech.*, vol. 38, pp. 629–637, 1990.

[35] R. J. Luebbers, K. S. Kunz, M. Schneider, and F. Hunsberger, "A finite-difference time-domain near zone to far zone transformation," *IEEE Trans. Antennas Propagat.*, vol. 39, pp. 429–433, 1991.

[36] P. M. Goorjian and A. Taflove, "Direct time integration of Maxwell's equations in nonlinear dispersive media for propagation and scattering of femtosecond electromag-netic solitons," *Optics Lett.*, vol. 17, pp. 180–182, 1992.

[37] R. W. Ziolkowski and J. B. Jerkins, "Full-wave vector Maxwell's equations modeling of self-focusing of ultra-short optical pulses in a nonlinear Kerr medium exhibiting a finite response time," *J. Optical Soc. America B*, vol. 10, pp. 186–198, 1993.

[38] R. M. Joseph and A. Taflove, "Spatial soliton deflection mechanism indicated by FDTD Maxwell's equations modeling," *IEEE Photonics Tech. Lett.*, vol. 2, pp. 1251–1254, 1994.

[39] W. L. Ko and R. Mittra, "A combination of FDTD and Prony's methods for analyzing microwave integrated circuits," *IEEE Trans. Microwave Theory Tech.*, vol. 39, pp. 2176–2181, 1991.

[40] J. A. Pereda, L. A. Vielva, and A. Prieto, "Computation of resonant frequencies and quality factors of open dielectric resonators by a combination of the finite-difference time-domain (FDTD) and Prony's methods," *IEEE Microwave Guided Wave Lett.*, vol. 2, pp. 431–433, 1992.

[41] J. Chen, C. Wu, T. K. Y. Lo, K.-L. Wu, and J. Litva, "Using linear and nonlinear predictors to improve the computational efficiency of the FDTD algorithm," *IEEE Trans. Microwave Theory Tech.*, vol. 42, pp. 1992–1997, 1994.

[42] V. Jandhyala, E. Michielssen, and R. Mittra, "FDTD signal extrapolation using the forward-backward autoregressive (AR) model," *IEEE Microwave Guided Wave Lett.*, vol. 4, pp. 163–165, 1994.

[43] S. Dey and R. Mittra, "Efficient computation of resonant frequencies and quality factors of cavities via a combination of the finite-difference time-domain technique and the Padé approximation," *IEEE Microwave Guided Wave Lett.*, vol. 8, pp. 415–417, 1998.

[44] W. Sui, D. A. Christensen, and C. H. Durney, "Extending the two-dimensional FDTD method to hybrid electromagnetic systems with active and passive lumped elements," *IEEE Trans. Microwave Theory Tech.*, vol. 40, pp. 724–730, 1992.

[45] B. Toland, B. Houshmand, and T. Itoh, "Modeling of nonlinear active regions with the FDTD method," *IEEE Microwave Guided Wave Lett.*, vol. 3, pp. 333–335, 1993.

[46] V. A. Thomas, M. E. Jones, M. J. Piket-May, A. Taflove, and E. Harrigan, "The use of SPICE lumped circuits as sub-grid models for FDTD high-speed electronic circuit design," *IEEE Microwave Guided Wave Lett.*, vol. 4, pp. 141–143, 1994.

[47] J. P. Berenger, "A perfectly matched layer for the absorption of electromagnetic waves," *J. Comp. Phys.*, vol. 114, pp. 185–200, 1994.

[48] D. S. Katz, E. T. Thiele, and A. Taflove, "Validation and extension to three dimensions of the Berenger PML absorbing boundary condition for FDTD meshes," *IEEE Microwave Guided Wave Lett.*, vol. 4, pp. 268–270, 1994.

[49] C. E. Reuter, R. M. Joseph, E. T. Thiele, D. S. Katz, and A. Taflove, "Ultrawideband absorbing boundary condition for termination of waveguiding structures in FDTD simulations," *IEEE Microwave Guided Wave Lett.*, vol. 4, pp. 344–346, 1994.

[50] Z. S. Sacks, D. M. Kingsland, R. Lee, and J. F. Lee, "A perfectly matched anisotropic absorber for use as an absorbing boundary condition," *IEEE Trans. Antennas Propagat.*, vol. 43, pp. 1460–1463, 1995.

[51] S. D. Gedney, "An anisotropic perfectly matched layer absorbing media for the truncation of FDTD lattices," *IEEE Trans. Antennas Propagat.*, vol. 44, pp. 1630–1639, 1996.

[52] R. W. Ziolkowski, J. M. Arnold, and D. M. Gogny, "Ultrafast pulse interactions with two-level atoms," *Phys. Rev. A*, vol. 52, pp. 3082–3094, 1995.

[53] A. S. Nagra and R. A. York, "FDTD analysis of wave propagation in nonlinear absorbing and gain media," *IEEE Trans. Antennas Propagat.*, vol. 46, pp. 334–340, 1998.

[54] Y. Huang, *Simulation of Semiconductor Materials Using FDTD Method*, M.S. thesis, Northwestern University, Evanston, IL, 2002.

[55] S.-H. Chang and A. Taflove, "Finite-difference time-domain model of lasing action in a four-level two-electron atomic system," *Optics Express*, vol. 12, pp. 3827–3833, 2004.

[56] M. Krumpholz and L. P. B. Katehi, "MRTD: New time-domain schemes based on multiresolution analysis," *IEEE Trans. Microwave Theory Tech.*, vol. 44, pp. 555–572, 1996.

[57] Q. H. Liu, *The PSTD Algorithm: A Time-Domain Method Requiring Only Two Grids Per Wavelength*, New Mexico State Univ., Las Cruces, NM, Tech. Rept. NMSU-ECE96-013, 1996.

[58] Q. H. Liu, "The pseudospectral time-domain (PSTD) method: A new algorithm for solutions of Maxwell's equations," *Proc. 1997 IEEE Antennas Propagat. Soc. Intl. Symp.*, vol. 1, pp. 122–125, 1997.

[59] O. M. Ramahi, "The complementary operators method in FDTD simulations," *IEEE Antennas Propagat. Mag.*, vol. 39, pp. 33–45, Dec. 1997.

[60] S. Dey and R. Mittra, "A locally conformal finite-difference time-domain algorithm for modeling three-dimensional perfectly conducting objects," *IEEE Microwave Guided Wave Lett.*, vol. 7, pp. 273–275, 1997.

[61] J. G. Maloney and M. P. Kesler, "Analysis of Periodic Structures," Chap. 6 in *Advances in Computational Electrodynamics: The Finite-Difference Time-Domain Method*, A. Taflove, (ed.), Norwood, MA: Artech House, 1998.

[62] J. B. Schneider and C. L. Wagner, "FDTD dispersion revisited: Faster-than-light propagation," *IEEE Microwave Guided Wave Lett.*, vol. 9, pp. 54–56, 1999.

[63] T. Namiki, "3-D ADI-FDTD method — Unconditionally stable time-domain algorithm for solving full vector Maxwell's equations," *IEEE Trans. Microwave Theory Tech.*, vol. 48, pp. 1743–1748, 2000.

[64] F. Zheng, Z. Chen, and J. Zhang, "Toward the development of a three-dimensional unconditionally stable finite-difference time-domain method," *IEEE Trans. Microwave Theory Tech.*, vol. 48, pp. 1550–1558, 2000.

[65] J. A. Roden and S. D. Gedney, "Convolutional PML (CPML): An efficient FDTD implementation of the CFS-PML for arbitrary media," *Microwave Optical Tech. Lett.*, vol. 27, pp. 334–339, 2000.

[66] T. Rylander and A. Bondeson, "Stable FDTD-FEM hybrid method for Maxwell's equations," *Comput. Phys. Comm.*, vol. 125, pp. 75–82, 2000.

[67] M. Hayakawa and T. Otsuyama, "FDTD analysis of ELF wave propagation in inhomogeneous subionospheric waveguide models," *ACES J.*, vol. 17, pp. 239–244, 2002.

[68] J. J. Simpson and A. Taflove, "Three-dimensional FDTD modeling of impulsive ELF propagation about the Earth-sphere," *IEEE Trans. Antennas Propagat.*, vol. 52, pp. 443–451, 2004.

[69] J. J. Simpson, R. P. Heikes, and A. Taflove, "FDTD modeling of a novel ELF radar for major oil deposits using a three-dimensional geodesic grid of the Earth-ionosphere waveguide," *IEEE Trans. Antennas Propagat.*, vol. 54, pp. 1734-1741, 2006.

[70] H. De Raedt, K. Michielsen, J. S. Kole, and M. T. Figge, "Solving the Maxwell equations by the Chebyshev method: A one-step finite difference time-domain algorithm," *IEEE Trans. Antennas Propagat.*, vol. 51, pp. 3155–3160, 2003.

[71] N. Chavannes, R. Tay, N. Nikoloski, and N. Kuster, "Suitability of FDTD-based TCAD tools for RF design of mobile phones," *IEEE Antennas Propagat. Magazine*, vol. 45, pp. 52–66, Dec. 2003.

[72] E. J. Bond, X. Li, S. C. Hagness, and B. D. Van Veen, "Microwave imaging via space-time beamforming for early detection of breast cancer," *IEEE Trans. Antennas Propagat.*, vol. 51, pp. 1690– 1705, 2003.

[73] J. J. Simpson, A. Taflove, J. A. Mix, and H. Heck, "Substrate integrated waveguides optimized for ultrahigh-speed digital inter-connects," *IEEE Trans. Microwave Theory Tech.*, vol. 54, pp. 1983-1990, 2006.

[74] H.-G. Park, S.-H. Kim, S.-H. Kwon, Y.-G. Ju, J.-K. Yang, J.-H. Baek, S.-B. Kim, and Y.-H. Lee, "Electrically driven single-cell photonic crystal laser," *Science*, vol. 305, pp. 1444–1447, 2004.

[75] L. Yin, V. K. Vlasko-Vlasov, A. Rydh, J. Pearson, U. Welp, S.-H. Chang, S. K. Gray, G. C. Schatz, D. B. Brown, and C. W. Kimball, "Surface plasmons at single nanoholes in Au films," *Applied Physics Lett.*, vol. 85, pp. 467–469, 2004.

[76] M. F. Yanik, S. Fan, M. Soljacic, and J. D. Joannopoulos, "All-optical transistor action with bistable switching in a photonic crystal cross-waveguide geometry," *Optics Lett.*, vol. 28, pp. 2506–2508, 2003.

[77] X. Li, A. Taflove, and V. Backman, "Recent progress in exact and reduced-order modeling of light-scattering properties of complex structures," *IEEE J. Selected Topics in Quantum Electronics, Special Issue on Biophotonics*, vol. 11, pp. 759-765, 2005.

[78] H. K. Roy, Y. Liu, R. Wali, Y. L. Kim, A. K. Kromine, M. J. Goldberg, and V. Backman, "Four-dimensional elastic light-scattering fingerprints as preneoplastic markers in the rat model of colon carcinogenesis," *Gastro-enterology*, vol. 126, pp. 1071–1081, 2004.

[79] H. K. Roy, Y. L. Kim, Y. Liu, R. K. Wali, M. J. Goldberg, V. Turhitsky, J. Horwitz, and V. Backman, "Risk-stratification of colon carcinogenesis through enhanced backscat-tering (EBS) spectroscopy analysis of the uninvolved colonic mucosa," *Clinical Cancer Research*, vol. 19, pp. 961–968, 2006.

[80] X. Li, "Synthesis of backscattering microscope amplitude images from FDTD-computed near fields," manuscript in preparation.

[81] Y. Liu, P. Pradhan, X. Li, Y. L. Kim, R. K. Wali, H. K. Roy, A. Taflove, and V. Backman, "Alteration of intracellular mesoscopic light transport in the earliest stage of carcinogenesis demonstrated by single-cell partial-wave spectroscopy," manuscript in preparation.

[82] S. H. Tseng, A. Taflove, D. Maitland, and V. Backman, "Pseudospectral time-domain simulations of multiple light scattering in three-dimensional macroscopic random media," *Radio Science*, vol. 41, RS4009, doi:10.1029/2005RS003408, 2006.

Allen Taflove is a professor in Northwestern University's EECS Department. He has helped to pioneer FDTD algorithms and applications since 1971. His publications include more than 115 journal papers and three editions (1995, 2000, and 2005) of the book *Computational Electrodynamics: The Finite-Difference Time-Domain Method*, which has become a standard reference in the FDTD field. He is listed by the Institute for Scientific Information as one of the most cited technical authors in the world.